Morphology−Interface−Property Relationships in Polystyrene/Ethylene−Propylene Rubber Blends. 1. Influence of Triblock Copolymer Interfacial Modifiers

Patrick Cigana and Basil D. Favis*

Centre de recherche appliquée sur les polymères, Ecole Polytechnique de Montréal, C. P. 6079, succ. Centre-Ville, Montréal, Québec, Canada H3C 3A7

Carolyne Albert and Toan Vu-Khanh

Département de Génie mécanique, Faculté des Sciences appliquées, Université de Sherbrooke, 2500, boul. de l'Université, Sherbrooke, Québec, Canada J1K 2R7

Received July 11, 1996; Revised Manuscript Received December 3, 1996[⊗]

ABSTRACT: Interfacial agents are often used to compatibilize immiscible polymer blends. They are known to reduce the interfacial tension, homogenize the morphology, and improve adhesion between phases. In this study, two triblock copolymers of styrene/ethylene−butylene/styrene (SEBS), of different molecular weights, were used to compatibilize a blend of 80 vol % polystyrene (PS) and 20% ethylene−propylene rubber (EPR). The emulsification curve, which relates the average minor phase particle diameter to the concentration of interfacial agent added, was used to quantify the effect of the interfacial agents on the blend morphology. Charpy and Izod impact tests were performed to determine the effect of the compatibilization on mechanical properties of the blend and to establish links between morphology, interface, and properties. Results suggest that for the lower molecular weight interfacial agent, a transition in fracture mechanisms, from fragile to ductile, occurs around 20% interfacial agent (based on the volume of the minor phase). This transition, however, is not observed with the high molecular weight interfacial agent.

Introduction

Blending existing polymers together has long been known to be an effective, low-cost way of developing novel materials. However, the vast majority of polymer pairs are mutually immiscible and, when blended, display very poor mechanical properties, due to their coarse, heterogeneous morphology and weak adhesion. In recent years, this problem has been addressed by incorporating a third component, or interfacial agent, into the incompatible blend.

Block copolymers have been shown to be effective interfacial agents for many incompatible blends of homopolymers. Each block of a diblock or multiblock copolymer is usually either miscible, or has strong affinities, with one of the two homopolymer phases. Thus, block copolymers can act by migrating to the interface between the homopolymers. It is believed that each block then localizes itself in its respective phase, thus reducing interfacial tension and promoting adhesion between phases.

Although the qualitative effect of the compatibilization of polymer blends is universally accepted, attempts to quantify these effects have gone in various directions. The emulsification curve, which has long been known in classical emulsions, is one method of quantifying the efficacy of interfacial agents in polymer blends.[1−3] This curve relates the average particle size of the minor phase to the concentration of interfacial agent added to the system. It is characterized by a sharp decrease in phase size at a low concentration of interfacial agent, followed by a leveling off to a near equilibrium diameter once a certain critical concentration has been reached. This concentration is believed to correspond to a point of saturation of the interface. The emulsification curve has recently been used in this group to compare the efficacy of different interfacial agents in a blend of polystyrene and ethylene−propylene rubber.[4,5]

Another way of monitoring the effect of the interfacial agent is by measuring the interfacial tension of the system with different concentrations of intefacial agent. This has been done recently by different authors.[6−8] Generally, the interfacial tension decreases with added emulsifying agent, until a certain concentration is reached, beyond which the interfacial tension remains nearly constant. Presumably, this phenomenon can, once again, be associated with interfacial saturation; once this critical concentration is reached, any added interfacial agent will not reach the interface but will be either dispersed in one of the two phases or form micelles,[9−11] hence the absence of effect on the interfacial tension or the dispersed particle size. Attempts have been made to localize the interfacial agent in the blends, but most have been either qualitative[12] or exploratory,[13] using a staining agent to identify the interfacial agent under transmission electron microscopy. It is essential, for a general better understanding of how interfacial agents act, that this problem be addressed in the near future.

Another important but still unclear aspect of the compatibilization of polymer blends is the relationship between morphology, the state of the interface, and mechanical properties. Willis et al.[1] studied a blend of reactive polystyrene and bromobutyl elastomer compatibilized with a liquid interfacial agent, 2-(dimethylamino)ethanol (DMAE). By using the emulsification curve in parallel with results of impact strength obtained at different concentrations of DMAE, they observed that despite a marginal effect on the morphology around the critical concentration, a sharp increase in impact strength occured after the critical concentration for emulsification had been reached. This suggests it is insufficient, as some authors have done,[14,15] to develop a model to predict the ideal particle size and interpar-

[⊗] Abstract published in *Advance ACS Abstracts,* May 15, 1997.

S0024-9297(96)00995-3 CCC: $14.00

ticle distance for optimal mechanical properties; one must also consider interfacial adhesion.

Creton et al.[16] used another approach, whereby they deposited the copolymer directly at the interface and measured the force required to separate the homopolymers from each other. They observed a mechanical reinforcement effect due to the presence of the copolymer at the interface. Their observations allowed them to develop a failure mechanism map,[17] which distinguishes two different regimes of failure at a compatibilized interface. If the block copolymer molecules themselves fail at the interface, the mechanism is known as chain scission. This can be expected to occur for long chains occupying the interface at a low areal density. Conversely, chain pull-out is more likely to occur with more densely packed, short interfacial agent chains.

The group of Bucknall and co-workers has done extensive work with various rubber-toughened polymer systems, such as HIPS/PPO blends,[18,19] ABS emulsion polymer,[20] PP/EPR,[21] and PA/EPR.[22] By using tensile dilatometry, they were able to separate the effects of shear-yielding and crazing phenomena in the tensile deformation of these blends.

The objective of this work is to relate the morphology and interfacial state of a modified polymer blend to the resulting mechanical properties, by combining the emulsification curve with a fracture mechanics approach.

Fracture Characterization

Although the global concept of fracture mechanics such as the strain energy release rate is unable to properly describe the fracture process,[23−27] it is presently widely used. On the other hand, in the Charpy and Izod tests, only the total energy absorbed by the sample to break can be measured, and it is well-known that this value does not directly correspond to the fracture performance of the material.[28−30]

Brittle fracture occurs when the strain energy stored in the sample up to the point of fracture is much larger than the energy dissipated in the creation of two fracture surfaces. The energy absorbed by the specimen to fracture is that which is elastically stored in the sample. In this type of fracture, the crack accelerates without any additional supply of energy by external forces. The crack grows in an unstable manner with a speed which is much greater than the impact speed. This leads to the phenomenon of shattering of the part in practice.

When a material exhibits a ductile mode of fracture, crack propagation occurs with much lower speed and in a much more stable manner than a brittle fracture. When crack propagation is stable, fracture can only occur with further supply of energy from external loads. This leads to the conclusion that with the same value of the critical strain energy release rate, G_c, and the fracture energy at crack initiation, G_i, the material exhibiting a ductile mode of fracture performs better in terms of impact resistance than a more brittle material.

For brittle fracture, the critical strain energy release rate, G_c, was determined as[28]

$$U = G_c BD\phi \tag{1}$$

where U is the energy absorbed by the sample, B and D are respectively the sample width and thickness and ϕ is a geometrical function which can be evaluated for any geometry by considering the appropriate calibration factor established for precracked samples.[15] From the slope of the plot of U versus $BD\phi$, using samples having different initial crack depths to vary ϕ, the fracture energy, G_c, can be obtained.

Table 1. Properties of Materials

material	commercial name	M_n (g/mol)	M_w (g/mol)	density (g/mL)	T_g (°C)
PS	Styron D685	125 000	275 400	1.05	108
EPR	Vistalon V-504	69 000	173 000	0.85	−38
K1	Kraton 1651	174 000		0.91	
K2	Kraton 1652	50 000		0.91	

For semiductile fracture, a mixed stable−unstable periods of crack propagation occurs in the same sample during impact fracture and in this case, the total energy absorbed by the sample to break, U, has been determined[29]

$$U = G_{st}A_1 + G_{inst}BD\phi_1 \tag{2}$$

where G_{st} is the average fracture energy during the first stable crack propagation stage, A_1 is the fracture surface area of the first stable crack propagation zone, G_{inst} is the fracture energy at the onset of unstable crack propagation, and ϕ_1 is the calibration factor corresponding to the crack length at the instability of crack propagation. By plotting U/A_1 against $BD\phi_1/A_1$, G_{st} and G_{inst} can be obtained respectively from the intercept and the slope of the straight line.

For the ductile fracture behavior, another approach taking into account the crack initiation and crack propagation energies in the material has been proposed.[30,31] Assuming that the fracture energy of the polymer with ductile behavior varies linearly with crack extension and is given by

$$G_r = G_i + T_a A \tag{3}$$

in which G_r is the actual fracture energy, G_i is the fracture energy at crack initiation, T_a represents the rate of change of G_r with crack extension, and A is the fracture surface. Since the energy absorbed by the specimen is mainly dissipated in the fracture process, the energy absorbed by the specimen becomes

$$U = \int_A G_r \, dA = G_i A + \frac{1}{2} T_a A^2 \tag{4}$$

From this equation one can obtain G_i by the intercept and T_a by the slope of the U/A versus A plot.

Experimental Section

Materials. The system investigated consists of a matrix of polystyrene (PS), supplied by Dow Chemical (Styron D685), and a minor phase of ethylene−propylene rubber (EPR), a random copolymer containing 54% ethylene, supplied by Exxon Chemical (Vistalon V-504). The interfacial agents were supplied by Shell: they consist of two styrene/ethylene−butylene/styrene (SEBS) triblock copolymers (Kraton 1651 and 1652, referred to as K1 and K2, respectively), containing 29% styrene. The number-average molecular weights of K1 and K2 are 174 000 and 50 000 g/mol, respectively. They are essentially monodisperse. The ethylene−butylene block contains about 35−40% polybutylene; the high polybutylene content inhibits the crystallization of the copolymer. Some properties of these materials are listed in Table 1.

Sample Preparation and Identification. The PS matrix and EPR minor phase were blended in volumetric proportions of 80:20. The matrix, minor phase, and interfacial agent were blended using a Leistritz AG twin-screw extruder, model 30.34 (L/D = 28) operating at 100 rpm. The temperature of the

Table 2. Injection Molding Conditions

temperature profile (°C)	240/230/210/180
mold temperature (°C)	60
injection pressure (bar)	145
injection speed (mm/s)	70 (20)
screw speed (rpm)	40 (35)
holding time (s)	10 (20)
holding pressure (bar)	50 (100)
back pressure (bar)	1
metering stroke (mm^{-1})	75 (45.5)
cooling time (s)	20 (60)

screws and the die was maintained at 200 °C. The extrudate was then quenched in cold water and granulated. Blends were prepared with interfacial agent concentrations of 0, 2.5, 5, 10, 15, 20, and 30% based on the minor phase. Thus, the sample denoted as K1 10 has the following composition: 80 parts PS, 20 parts EPR, and 2 parts (10% of EPR content) Kraton 1651. Likewise, K2 20 has a composition of 80 parts PS, 20 parts EPR, and 4 parts (20% of EPR content) Kraton 1652. About 0.1% by weight of Irganox 1010 antioxidant (Ciba-Geigy) was also added to the blends.

The granules were then molded into 6 mm thick plates using a Battenfeld 80-ton injection molding machine, equipped with a Unilog 8000 interface. Injection molding conditions are given in Table 2.

Morphological Analysis. Emulsification curves were obtained for blends prepared in a Brabender internal mixer. The components were blended for 8 min, at 50 rpm and a temperature of 200 °C, before being quenched in cool water. Plane surfaces were obtained for each sample using a Leica model Jung RM 2065 microtome equipped with a glass knife. Samples were held under −100 °C with a stream of liquid nitrogen to minimize surface deformation while cutting. Extraction of the minor phase with a solvent was not required; it appears that the rubber particles are ejected from the matrix during microtomy. This may be due to a large difference between the thermal expansion coefficients of the two components.

The samples were then coated with a thin gold−palladium layer prior to scanning electron microscopy (SEM). Micrographs were taken using a JEOL model T300 scanning electron microscope at 10.0 kV. Diameters were determined from surface area measurements, using a semiautomatic analysis method, developed in-house and described elsewhere.[32] For each sample, the number-average diameter, d_n, and volume average diameter, d_v, were calculated from at least 250 individual particle measurements. A correction procedure was applied to account for polydispersity and for the fact that the knife rarely cuts through the particles at their equator. This procedure was developed by Saltikov.[33]

SEM observation in the longitudinal direction of the injection molded samples revealed that they display a distinct skin/core progression in the morphology. The EPR particles are highly elongated through the first 0.8−1.2 mm of the samples, at which point a few spherical particles appear. This transition from elongated to spherical particles occurs through the next 0.4 mm, after which nearly all the particles are approximately spherical (core). This skin/core morphology did not seem to depend on the amount of interfacial modifier.

Tensile Tests. Traction tests at a loading rate of 10 mm/min were performed on an Instron automated material testing system, Model 4306. The samples used for these tests were injection-molded dog-bone specimens with a thickness of 3.11 mm, width of 9.9 mm, and gauge length of 85 mm. These tests were carried out at room temperature.

Impact Tests. Three-point-bending impact tests (Charpy tests) were done on a Monsanto plastic impact machine. The calculated hammer speed at the beginning of the impact was 2.5 m/s. The samples were cut out of 6-mm-thick plates to a length and width of 50 mm and 10 mm, respectively, using a ribbon saw. The initial crack created in the specimen had a length varying between 11% and 79% of specimen width. A prenotch was first made with a ribbon saw and the final cut was done by forcing a razor blade into the specimen with a vise. To reduce the bouncing effect of the sample on the striker during impact, a small amount of plasticine was placed on the striker. The tests were carried out at room temperature and with a humidity of about 50%.

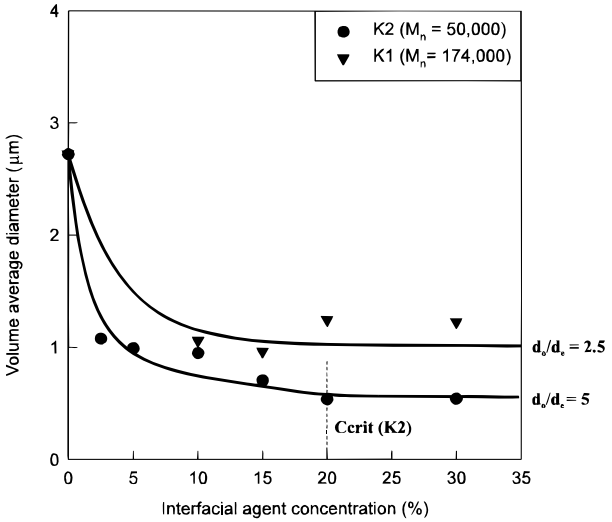

Figure 1. Emulsification curves for blends of 80% polystyrene and 20% ethylene−propylene rubber (volumetric), compatibilized with Kraton 1651 (▼) and Kraton 1652 (●). The interfacial agent concentrations are based on the volume of the minor phase (e.g. blend K2 20 contains 80 parts PS, 20 parts EPR and 4 parts K2, which represents 20% of EPR content). The blends were produced on a Brabender mixer.

Unnotched Izod impact tests were also performed on rectangular samples of 12 mm by 60 mm, also cut out from these injection-molded 6 mm thick plates. The tests were done on a Custom Scientific Instruments model CS-137C impact tester, equipped with a 923 g pendulum.

Results and Discussion

Morphology. The emulsifying effect of the interfacial agents used in this work is shown in Figure 1. Clearly, the lower molecular weight interfacial agent, K2, is more effective at reducing the particle size than the high molecular weight copolymer, K1. In the first case, the volume average particle size is reduced from 2.72 to around 0.55 μm, a decrease of nearly 80%, whereas the K1 triblock copolymer only decreased it to about 1.1 μm. The greater spread observed in the K1 data is an additional indication of its poorer emulsifying ability.

These results, though in apparent contradiction with previous work performed in this group[4] which showed that the emulsification capacity of triblock copolymers was independent of their molecular weight, can be explained by the fact that the present work was performed at 20% minor phase instead of 10%. Since the concentration of interfacial agent is expressed based on the volume of the minor phase, there is, for a given concentration, twice as much interfacial agent in an 80:20 blend than in a 90:10 blend. This probably results in much of the interfacial agent being "lost" in the matrix in the form of micelles or free molecules. These "losses" can be expected to be higher for the high molecular weight material, since large molecules form micelles more readily than smaller ones.[35] It is thus resonable to assume that, at least in the case of K1, much of the interfacial agent does not find its way to the interface. In addition, injection-molded samples have been subjected to annealing at 200 °C for 100 min. Figure 2 shows micrographs of the K1- and K2-modified blends containing 30% interfacial agent (based on the minor phase), before and after the annealing process.

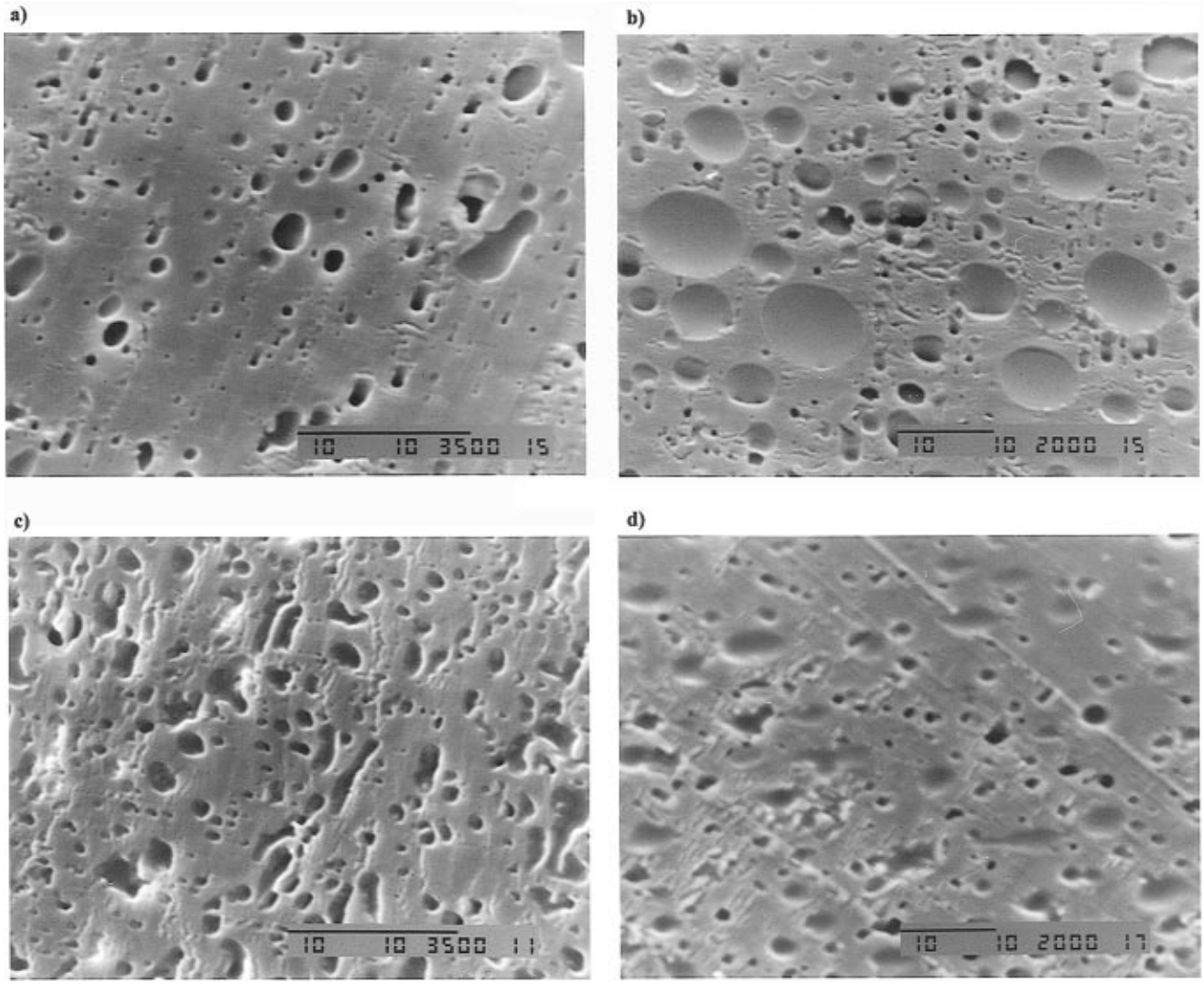

Figure 2. Micrographs of injection-molded blends of PS/EPR/K1 and K2, containing 30% of emulsifier based on the minor phase (blend composition 80 parts PS, 20 parts EPR, 6 parts interfacial modifier). (a) K1 30, before annealing (magnification: 3500×); (b) K1 30, after annealing (magnification: 2000×); (c) K2 30, before annealing (magnification: 3500×); (d) K2 30, after annealing (magnification: 2000×). Scale bars in all cases: 10 μm.

Much coalescence was observed for samples compatibilized by K1; image analysis was carried out on these micrographs and the volume average particle diameter increase upon annealing was found to be a factor 4.2 for the K1-compatibilized samples, and a factor 2.2 for the K2-compatibilized samples. This is a further indication that much of the K1 is not at the interface.

Tensile Properties. Displacement at break, maximum loads, and total energy absorbed were measured for all blends. The samples showed an elongation at break between 4 and 6 mm. Most samples showed a striction point (maximum load) around 1.3 kN and a total energy absorbed at the point of fracture between 4 and 5 J. The samples compatibilized by K2 showed a slightly higher elongation at break and total energy at break, but overall, the interfacial modifier had very little effect on the tensile properties.

Impact. Polymers can break in distinct manners under impact. The type of fracture can be characterized from the amount of plastic deformation at the crack tip and the stability of crack propagation.

Many observations can help distinguish whether a fracture occurred in a ductile or fragile manner. The first one is the observation of the specimen's trajectory after its fracture. When a fracture is brittle, the sample generally breaks into two halves that fly away after fracture. When the sample breaks in a ductile manner, the two halves remain attached by a thin ligament and are pushed away by the hammer at a much lower velocity.

The second technique is based on the observation of the fracture surface. An unstable crack propagation leads to a rough surface often showing a branching effect. When stable fracture occurs, the surface exhibits a whitening effect or could become bright, reflecting light, due to craze formation.

Figure 3 shows the load vs deflection curve for a brittle sample. The load vs deflection curve for a more ductile specimen is shown in Figure 4. From these impact tests it was determined that all the samples fracture in an unstable manner except those containing 20% or more of the K_2 interfacial agent. Only the K2 20 and the K2 30 samples had a ductile fracture. For the specimens with brittle fracture, the U vs $BD\phi$ curve was drawn to determine G_c. Such a curve is shown in Figure 5. For ductile specimens, the values of G_i, the fracture energy at crack initiation, was determined by plotting the U/A vs A curves. An example of that plot is shown in Figure 6. Strain energy release rates and fracture energies at crack initiation are plotted as a

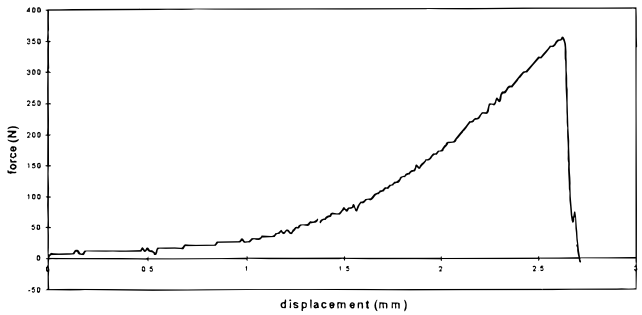

Figure 3. Typical load-deflection curve for a brittle sample.

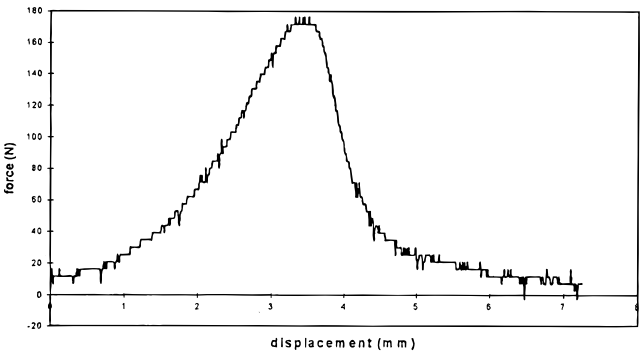

Figure 4. Typical load-deflection curve for a ductile sample.

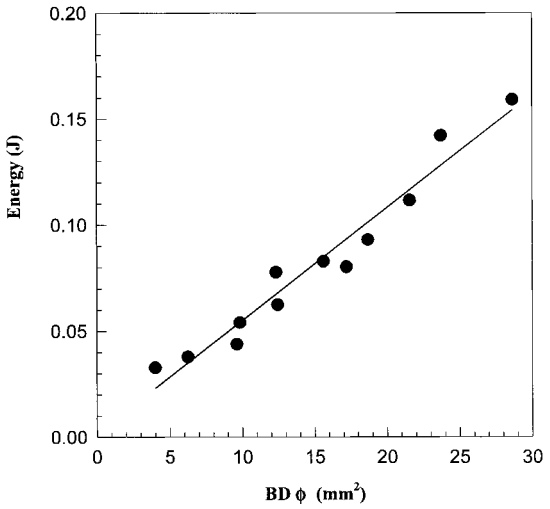

Figure 5. Determination of G_c for specimens that showed brittle fracture.

Table 3. Values of G_i and T_a for Blends with Ductile Fracture

sample	G_i (kJ/m^2)	T_a (kJ/m^4)
K2 20	6.4	-2×10^{-5}
K2 30	7.3	-3×10^{-5}

function of concentration of interfacial modifier in Figure 7. Table 3 shows a comparison of G_i and T_a for the blends with ductile fracture.

A distinct effect is observed, for the blends compatibilized by K2, above 15% interfacial modifier (based on the minor phase). A transition from fragile to ductile rupture, along with the corresponding increase in impact strength, can clearly be seen. This transition seems to occur at a concentration of interfacial modifier equal to the critical concentration for emulsification for this blend (see Figure 1) and likely corresponds to a state of interfacial saturation. It is interesting to note that for the blends modified by K1, the high molecular weight compatibilizer, a very different behavior is

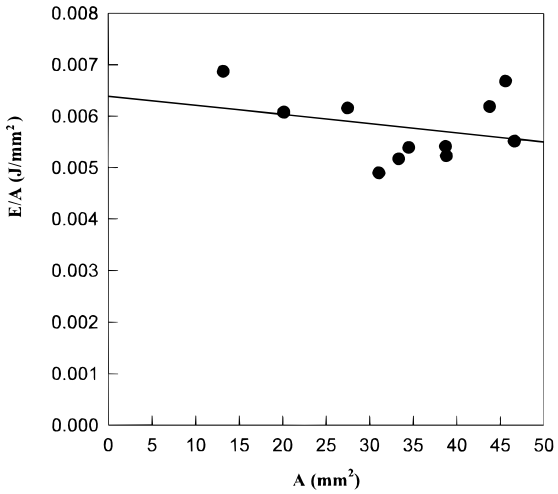

Figure 6. Determination of G_i for specimens that showed stable crack propagation (ductile fracture).

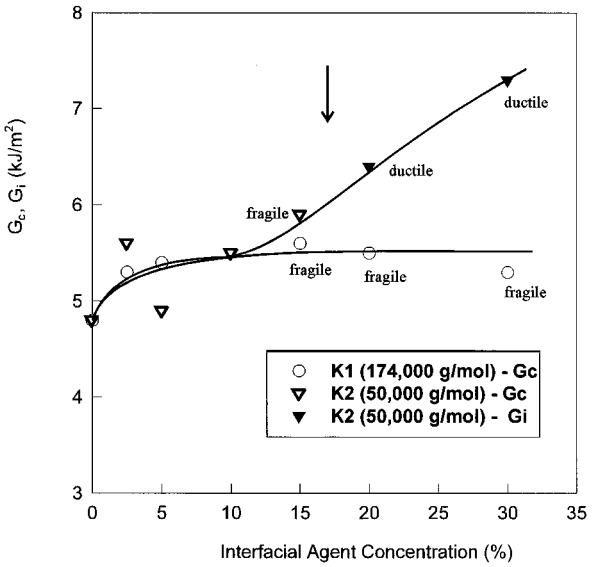

Figure 7. Results of the Charpy impact tests for blends of 80% PS and 20% EPR, compatibilized by Kraton 1651 (○) and Kraton 1652 (▼, ▽). Values of G_c are reported for blends with brittle fracture; values of G_i are reported for the two blends (K2 20 and K2 30) that showed stable crack propagation (ductile fracture). The arrow shows the approximate point of transition between fragile and ductile fracture mechanisms, near the critical concentration for emulsification (see Figure 1).

observed; the addition of modifier results in a very little increase in impact strength. Moreover, this increase is nearly independent of compatibilizer concentration. There is no brittle−ductile transition: all samples showed a fragile mode of fracture.

The results of the unnotched Izod impact tests are shown in Figure 8. In spite of the rather large standard deviations observed for certain blends, the same general trends can be observed as with the Charpy impact tests: for K1, the high molecular weight interfacial agent, the increase in impact strength is marginal and does not depend on the concentration of interfacial agent. With the low molecular weight interfacial agent, K2, the improvement is more marked, especially for the blends containing 20 and 30% interfacial agent. The fact that both the notched (Charpy) and unnotched (Izod) samples exhibit the same behavior indicates that the results are truly bulk properties and are not dependent on the skin properties nor on the crack tip.

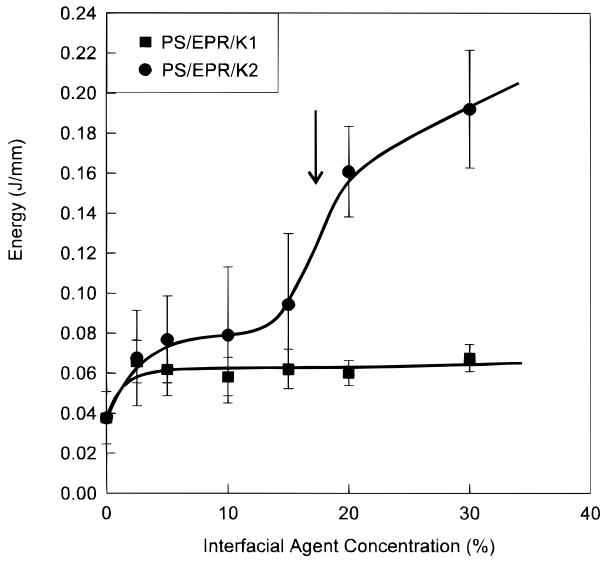

Figure 8. Results of the Izod impact tests for blends of 80% PS and 20% EPR, compatibilized with Kraton 1651 (■) and Kraton 1652 (●). As with the Charpy impact results, a significant effect is observed for K2 20 and K2 30 blends.

These results can be readily explained in light of the morphological analysis. Since the high molecular weight interfacial agent, K1, does not effectively migrate to the interface, as shown by the emulsification curve, the interface is not saturated, adhesion is poor, and the stress cannot be transfered effectively from the polystyrene to the rubber phase. The interface is weak, and the samples break in a brittle way, with a low toughness. The K2, in spite of its short chains and low molecular weight (only 7500 g/mol for each of the styrene blocks), does saturate the interface and provides an effective stress transfer across the interface, resulting in a ductile fracture mechanism once saturation has been attained (20% interfacial agent in this case). It should be noted that throughout the K2 emulsification curve, the change in particle size, though measurable, is relatively small. For example, the volume average diameter decreases by less than 25% between the blends compatibilized by 15% K2 and 30% K2; nevertheless, the change in impact strength and fracture mechanism is remarkable. The observed effects must therefore be attributed to an important change in the state of the interface rather than a morphological effect.

Other authors have also observed an effect of the molecular weight of the interfacial agent on mechanical properties. Char et al.[35] studied a laminar system comprised of two plates of poly(phenylene oxide) and poly(methyl methacrylate), compatibilized by a layer of PS−PMMA diblock copolymer. By varying the molecular weight of the diblock, they determined an optimum molecular weight (around 80 000 g/mol) at which highest toughness can be achieved. They explained the subsequent decrease in toughness with higher molecular weight compatibilizers by a transition in interfacial failure regimes. Creton et al.[36] distinguished two regimes. If the chain surface density is low, but the chains are long (this would be the case for high molecular weight compatibilizers), then failure would occur in the "joint region", i.e. at the A−B transition in the block copolymer. The failure would then be of the "chain-scission" type, and brittle fracture would be observed. If the chain surface density is high, but the chains are short (low molecular weight modifier), failure will occur in the "brush region", between the A block and the A homopolymer. The interface would then fail by chain pullout, which would involve some plastic deformation (ductile fracture). It must be kept in mind that in those studies, the interfacial agent was placed directly at the interface; molecular migration was not a variable, and the observed effects could be explained by such interfacial failure regime arguments. This work introduces another possible explanation for the decrease in toughness with increasing molecular weight, which may be especially applicable to typical melt blending processes; it is possible that much of the interfacial agent does not actually reach the interface.

Future work will compare the efficacies of diblock and triblock copolymers.

Conclusions

A morphological analysis and a fracture mechanics approach were combined to determine the effect of the compatibilization of PS/EPR blends by addition of styrene/ethylene−butylene/styrene triblock copolymers. For blends compatibilized by the low molecular weight copolymer (50 000 g/mol), the Izod impact strength increased 4−5-fold at interfacial agent concentrations above the critical concentration for emulsification. Charpy impact tests also showed that for those samples, a transition from fragile to ductile fracture mode occurred.

Although, intuitively, it may be expected that the higher molecular weight copolymer (174 000 g/mol) would have given a blend with better mechanical properties because of deeper anchoring of the interfacial agent into each of the phases, the opposite effect was observed. The Izod and Charpy impact strengths of blends compatibilized by K1 showed only marginal increase, and no brittle−ductile transition was observed; all samples broke in a fragile mode. Detailed morphological analysis showed that the high molecular weight copolymer was not an efficient emulsifier, and it is believed that it does not migrate effectively to the interface; this explains its incapacity to improve the blend toughness in a significant way.

Acknowledgment. The authors would like to thank the Natural Science and Engineering Research Council of Canada for their financial support, as well as Stephen Odje and Magella Tremblay from the University of Sherbrooke. One author (P.C.) wishes to thank Valérie Benoit and Alain Tremblay for their contributions and Christophe Pagnoulle for fruitful discussions.

References and Notes

(1) Willis, J. M.; Favis, B. D. *Polym. Eng. Sci.* **1988**, *28*, 1416.
(2) Willis, J. M.; Favis, B. D.; Lunt, J. *Polym. Eng. Sci.* **1990**, *30*, 1073.
(3) Favis, B. D. *Polymer* **1994**, *35*, 1552.
(4) Matos, M.; Favis, B. D.; Lomellini, P. *Polymer* **1995**, *36*, 3899.
(5) Cigana, P.; Favis, B. D.; Jérôme, R. *J. Polym. Sci., Polym. Phys. Ed.* **1996**, *34*, 1691.
(6) Wagner, M.; Wolf, B. A. *Polymer* **1993**, *34*, 1460.
(7) Hu, W.; Koberstein, J. T.; Lingelser, J. P.; Gallot, Y. *Macromolecules* **1995**, *28*, 5209.
(8) Chapleau, N.; Favis, B. D.; Carreau, P. J. *Proc. Am. Chem. Soc. Div. Polym. Mat. Sci. Eng.* **1995**, 18.
(9) Noolandi, J.; Hong, M. K. *Macromolecules* **1982**, *15*, 482.
(10) Noolandi, J. *Polym. Eng. Sci.* **1984**, *24*, 70.
(11) Vilgis, T. A.; Noolandi, J. *Macromolecules* **1990**, *23*, 2941.
(12) Fayt, R.; Jérôme, R.; Teyssié, Ph. *J. Polym. Sci., Polym. Lett. Ed.* **1986**, *24*, 25.
(13) Tremblay, A.; Tremblay, S.; Favis, B. D.; Selmani, A.; L'Espérance, G. *Macromolecules* **1995**, *28*, 4771.
(14) Wu, S. *Polymer* **1985**, *26*, 1855.

(15) Jiang, W.; Liang, H.; Zhang, J.; He, D.; Jiang, B. *J. Appl. Polym. Sci.* **1995**, *58*, 537.
(16) Creton, C.; Kramer, E. J.; Hui, C.; Brown, H. R. *Macromolecules* **1992**, *25*, 3075.
(17) Washiyama, J.; Kramer, E. J.; Creton, C. F.; Hui, C. *Macromolecules* **1994**, *27*, 2019.
(18) Bucknall, C. B.; Clayton, D.; Keast, W. E. *J. Mater. Sci.* **1972**, *7*, 1443.
(19) Bucknall, C. B.; Clayton, D.; Keast, W. *J. Mater. Sci.* **1973**, *8*, 514.
(20) Bucknall, C. B.; Drinkwater, I. C. *J. Mater. Sci.* **1973**, *8*, 1800.
(21) Bucknall, C. B.; Page, C. J. *J. Mater. Sci.* **1982**, *17*, 808.
(22) Bucknall, C. B.; Heather, P. S.; Lazzeri, A. *J. Mater. Sci.* **1989**, *16*, 2255.
(23) Sih, G. C.; MacDonald, B. *Eng. Fract. Mech.* **1974**, *6*, 361.
(24) Sih, G. C. *Eng. Fract. Mech.* **1983**, *5*, 365.
(25) Sih, G. C.; Madenci, E. *Eng. Fract. Mech.* **1983**, *18*, 1159.
(26) Gdoutos, E. E.; Sih, G. C. *Theor. Appl. Fract. Mech.* **1984**, *3*, 95.
(27) Vu-Khanh, T.; Fisa, B. *Theor. Appl. Fract. Mech.* **1990**, *13*, 11.
(28) Plati, E.; Williams, J. G. *Polym. Eng. Sci.* **1975**, *15*, 470.
(29) Vu-Khanh, T.; de Charentenay, F. X. *Polym. Eng. Sci.* **1985**, *25*, 841.
(30) Vu-Khanh, T. *Polymer* **1988**, *29*, 1979.
(31) Vu-Khanh, T. *Theor. Appl. Fract. Mech.* **1994**, *21*, 83.
(32) Favis, B. D.; Chalifoux, J. P.; *Polym. Eng. Sci.* **1987**, *27*, 1591.
(33) Saltikov, S. A. *Proceedings of the 2nd International Congress Stereology* H. Elias: New York, 1967.
(34) Whitmore, M. D.; Noolandi, J. *Macromolecules* **1985**, *18*, 657.
(35) Char, K.; Brown, H. R.; Deline, V. R. *Macromolecules* **1993**, *26*, 4164.
(36) Creton, C.; Brown, H. R.; Deline, V. R. *Macromolecules* **1994**, *27*, 1774.

MA960995Z